IEEE Access
Multidisciplinary ⋮ Rapid Review ⋮ Open Access Journal

Received March 13, 2020, accepted April 6, 2020, date of publication April 14, 2020, date of current version April 30, 2020.

Digital Object Identifier 10.1109/ACCESS.2020.2987928

A Reliability-Aware Joint Design Method of Application Mapping and Wavelength Assignment for WDM-Based Silicon Photonic Interconnects on Chip

HUI LI[1], (Member, IEEE), FEIYANG LIU[2], HUAXI GU[1], ZHUQIN CHU[1], AND XIAOCHUN YE[3]
[1]State Key Laboratory of Integrated Services Networks, School of Telecommunications Engineering, Xidian University, Xi'an 710071, China
[2]Xi'an Aeronautics Computing Technique Research Institute, AVIC, Xi'an 710065, China
[3]State Key Laboratory of Computer Architecture, Institute of Computing Technology, Chinese Academy of Sciences, Beijing 100190, China

Corresponding author: Huaxi Gu (hxgu@xidian.edu.cn)

This work was supported in part by the National Natural Science Foundation of China under Grant 61802290, in part by the National Key Research and Development Program of China under Grant 2018YFE0202800, in part by the National Natural Science Foundation of China under Grant 61634004 and Grant 61934002, in part by the Fundamental Research Funds for the Central Universities under Grant XJS200101, in part by the HKKXJJ under Grant 2018ZC31002, in part by the Open Project Program of the State Key Laboratory of Mathematical Engineering and Advanced Computing under Grant 2019A01, in part by the State Key Laboratory of Computer Architecture under Grant CARCH201707, and in part by the Natural Science Foundation of Shaanxi Province for Distinguished Young Scholars under Grant 2020JC-26.

ABSTRACT Silicon photonic interconnects on chip is an emerging technology for future ultra-scale and data-intensive computing chips, e.g., many-core processors, owing to its high transmission speed and low latency. However, in the Wavelength Division Multiplexing (WDM)-based architecture, the communication reliability can be significantly affected by the signal losses and crosstalk, due to the inherent characteristic of photonic devices. This paper studies the influence on reliability of managing application mapping and wavelength assignment separately. To deal with this issue, we propose a reliability-aware joint design method coordinating application mapping and wavelength assignment schemes. For a given application core graph and a network architecture, the design method can obtain a result of application mapping and wavelength assignment with improved reliability, compared to the separate scheme. According to the evaluation of Optical Signal-to-Noise Ratio (OSNR), the proposed method enables more reliable communication under given applications.

INDEX TERMS Silicon photonic interconnects on chip, design method, reliability, application mapping, wavelength assignment.

I. INTRODUCTION

Silicon photonic interconnects on chip is promising to improve the communication performance of the future multi-/many-core processors, providing high transmission speed and low latency for high-performance computing applications [1]. The development of silicon photonics makes it possible to integrate the required photonic devices, such as lasers, modulators, waveguides, and photodetectors, onto one single chip [2], [3]. At the same time, CMOS-compatible fabrication process allows photonic devices to be integrated with electrical interconnects, which is fundamental for future mass production.

In silicon photonic interconnects on chip, data is transmitted in optical waveguides in the form of optical signals. With WDM technology, multiple optical signals at different wavelengths can be delivered at the same time in one optical waveguide. This technology mainly relies on Microring Resonators (MRs) at different resonant wavelengths, which are utilized for modulating, routing, and filtering the optical signals based on the resonant wavelengths and signal wavelengths [4]. Compared to the manner of single-wavelength communication, the WDM-based communication can improve the communication bandwidth by N_{WL} times [5], with N_{WL} available wavelengths.

The associate editor coordinating the review of this manuscript and approving it for publication was Gian Domenico Licciardo.

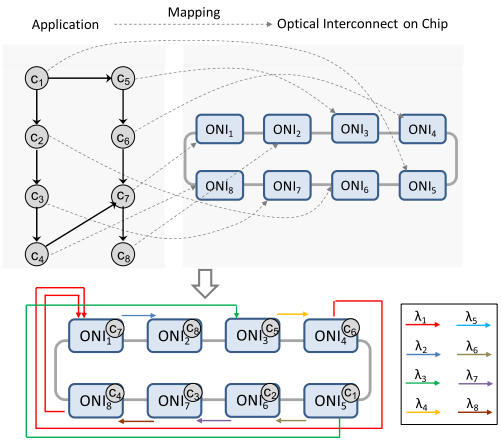

FIGURE 1. An instance of application mapping in optical interconnects on chip, with destination-based wavelength assignment [11] in consideration of the clockwise transmission.

In the WDM-based silicon photonic interconnects on chip, the communications in parallel between different pairs of source and destination nodes are specified by different resonant wavelengths. To utilize more wavelengths in optical communications can provide higher bandwidth. However, the coupling of optical signal at the MRs is not perfect. When the parallel communications at different wavelengths have some overlap with each other along the whole paths, the received signals at the destination side not only experience the optical losses unavoidably induced by the optical devices, but also can be affected by the crosstalk from other optical signals at different wavelengths. As a result, the OSNR of the expected signal would decrease, and thus the communication reliability would get worse, especially when many wavelengths are used for communication. In the worst case, the received signal might not be good enough for the correct communication [6], which leads to more laser power consumption [7], [8] for re-transmitting or more cost for signal correction. In the meantime, the scalability of photonic interconnect architecture is limited under a given laser power budget. Thus, to improve the OSNR is in turn possible to improve the power efficiency and the scalability.

Application mapping and wavelength assignment are two crucial aspects needed to be concerned. Firstly, the mapping result of a specific application can affect the relative locations of parallel communications in a network architecture, which thus influences the losses and crosstalk to an expected signal. Improper application mapping has a negative influence on the communication performance and reliability, which in return increases the laser power consumption [9]. For instance, an improper mapping result with the destination-based wavelength assignment is shown as the example in Figure 1. The communication $c_6 \rightarrow c_7$ experiences long routing path, leading to large signal losses. And the communication $c_4 \rightarrow c_7$ has overlap with two other communications (i.e., $c_6 \rightarrow c_7$ and $c_1 \rightarrow c_5$), resulting in large crosstalk for itself. Secondly, the wavelength assignment scheme can influence the crosstalk. For instance, if two adjacent wavelengths are assigned along one same optical path, the crosstalk can be greatly increased due to inevitable inter-coupling. In addition, different wavelength channel spacing can lead to different influences on the reliability [10]. So, different wavelength assignments for the specific communications, especially for the parallel ones, have different influences on the communication reliability in WDM-based architectures. For instance, the communication reliability under the source-based wavelength assignment would vary [11] for the application mapping result in Figure 1.

However, **the result of application mapping is based on a given wavelength assignment, while the result of wavelength assignment depends on a given application mapping result**. If the application mapping or the wavelength assignment is managed separately, high signal loss and high crosstalk would be resulted into. Thus, in this work, we propose a reliability-aware joint design method of application mapping and wavelength assignment for the WDM-based silicon photonic interconnects on chip, based on reliability analysis model. The main contribution of this work is summarized as follows.

- A joint design method is proposed by taking into consideration of both application mapping and wavelength assignment, to reduce the signal loss and crosstalk, thereby improving the communication reliability. The correlation of application mapping and wavelength assignment is studied for the first time, to our knowledge.
- A reliability-aware application mapping scheme and a reliability-aware wavelength assignment scheme are designed, based on our reliability model. In this model, the transmission property of MR is used for the loss and crosstalk evaluation.
- The method is designed to be adaptable for different topologies and applications, with the flexibility of employing different optimization algorithms. In this work, ant colony optimization algorithm (ACO) is used for the illustration.

The rest of this paper is structured as follows. Section II presents the related work. Then, the network architecture and the reliability problem are described in Section III. Section IV presents the proposed reliability-aware joint design method. Section V details the proposed application mapping scheme and Section VI shows the wavelength assignment scheme. Section VII presents the OSNR model and Section VIII gives the case study and evaluation results. Section IX concludes the paper.

II. RELATED WORK

In this paper, the research on crosstalk-induced reliability issue is carried out in the WDM-based silicon photonic interconnects on chip, especially in the aspects of problem formation and solution.

In the aspect of **problem formulation**, the existing research mainly focuses on the crosstalk model of WDM-based silicon photonic interconnects [12]–[17]. For instance, the OSNR of a ring-based Optical Networks-on-Chip (ONoC) and the crosstalk of a WDM-based ONoC are studied in [12] and [13] respectively, by considering fixed loss values of photonic devices from the state-of-art work as in [17]. These models can show a quantitative connection among the communication reliability, the crosstalk, and the scalability (detailed in Table 1 including ONoCs by using both single wavelength and multiple wavelengths). However, the influences of application property and wavelength assignment are not concerned.

In the aspect of **solution to mitigate the influence**, existing research mainly focuses on the architecture design [18], the system-level management schemes (e.g., DVFS, workload monitoring) [19], application mapping [20], [21], adaptive laser power control [22], redundant MRs and encoding [23], multilevel signaling [24], increase of wavelength spacing [25], wavelength allocation [9], etc. For instance, in [20], [21], an application mapping scheme is employed to reduce the worst-case crosstalk in the manner of reducing the number of communications in one waveguide, based on the pre-defined communication pattern of specific application. However, fixed loss values of photonic devices are considered in the work, and the influence of wavelength assignment is not considered, which would increase the crosstalk. In [22], an adaptive power control technique is used for the inter/intra-chip network to enhance OSNR. It can improve the laser power efficiency by allocating appropriate power strength when the communication pattern and routing path are both determined. In [23], double MRs and data encoding are employed to reduce crosstalk. In [24], four-amplitude-level optical signals are used to improve the reliability and energy efficiency. In [25], the OSNR is improved by reducing the number of multiplexed wavelengths, indicating that the increase of wavelength spacing between two adjacent wavelengths can lead to the reduced crosstalk. Besides, some other approaches such as stochastic communication (or probabilistic flooding protocols), network coding, and reconfiguration in electrical NoCs [26]–[28] can be considered for the solution reference.

However, wavelength assignment is not taken into account in the existing schemes, i.e., power control and increase of wavelength spacing [22], [25]. A wavelength allocation scheme based on genetic algorithm is proposed in [9] to achieve a trade-off between performance and energy cost. This scheme mainly focuses on the optimization in the number of communication wavelengths, without the consideration of the wavelength spacing and the overlapping communications. Also, the communication case where each communication is performed on one wavelength is pointed out to be the most energy efficient [9]. In our work, the wavelength assignment scheme is designed under this case.

In addition, several static wavelength assignment schemes are proposed, e.g., source-based wavelength assignment [11], destination-based wavelength assignment [11], and communication-based wavelength assignment [29]. However, the influence of wavelength assignment on reliability is not considered.

In our proposed method, the application mapping and wavelength assignment are combined to improve the communication reliability at design time.

TABLE 1. Related research on the communication reliability and network scalability.

Type	Topology	Optical router	Network scale ($OSNR_{wc}$)
ONoCs by using one single wavelength	Mesh [14][15]	Optimized Crossbar	6×6 (3.5dB) 16×16 (-13.9dB)
		Crux	6×6 (4.8dB) 16×16 (-2.4dB)
	Folded-Torus [15]	Optimized Crossbar	14×14 (-1.8dB)
		Crux	14×14 (-0.2dB)
	Fat-Tree [16]	OTAR	128 (-17.3dB)
WDM-based ONoCs by using multiple wavelengths (e.g., 16 wavelengths)	Mesh [13]	Crux	64 (-1.7dB) 128 (-10.8dB)
	Folded-Torus [13]	Crux	64 (-0.1dB) 128 (-7.1dB)
	Fat-Tree [13]	OTAR	64 (0.9dB) 128 (-9dB)

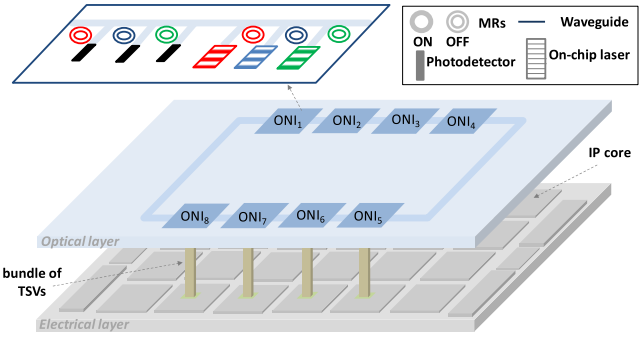

FIGURE 2. A 3D network architecture, implemented with CHAMELEON [30] at the optical layer, connecting IP cores at the electrical layer with TSVs.

III. RELIABILITY PROBLEM IN WDM-BASED SILICON PHOTONIC INTERCONNECTS ON CHIP

This section illustrates the reliability problem in WDM-based silicon photonic interconnects on chip based on the wavelength routing

Figure 2 illustrates a 3D network architecture to demonstrate the proposed method, as well as the case study. It is composed of i) an electrical layer implementing processing cores (in tiles) and memories, and ii) an optical layer with the implementation of CHAMELEON [30]. The activities of processing cores lead to both local and global communications which are realized by electrical interconnects in the electrical layer and photonic interconnects in the optical layer, respectively. The communication hierarchy is defined at design time, and depends mainly on the total number of processing cores and the complexity and bandwidth of photonic interconnects. Note that the proposed method is applicable for other

network architectures as well, while CHAMELEON is used for the demonstration of the proposed method.

The silicon photonic fabrication process is CMOS-compatible, and it allows integrating the required photonic devices, such as on-chip lasers, waveguides, MRs, and photodetectors. The silicon photonic devices (e.g., MRs) are mostly wavelength-selective, enabling the WDM technology and wavelength routing for high-bandwidth communication. These devices are assembled into so-called Optical Network Interfaces (ONIs), which are responsible for emitting the light, modulating optical signals with the data to be transmitted, and receiving them on the destination side (as shown in Figure 2). All the ONIs are connected via a ring bus waveguide propagating optical signals. Vertical-Cavity Surface-Emitting Lasers (VCSELs) and photodetectors are respectively connected to CMOS drivers and CMOS receivers through TSVs [6]. Multiple wavelengths are utilized at the optical layer for communications, enabled by MRs at different resonant wavelengths. CHAMELEON is implemented at the optical layer, and it is a ring-based network allowing reconfigurable communications between source and destination, with active MRs in ONIs. Also, it demonstrates less laser output power [30] compared to related optical crossbars including Snake [31] and SWMR (Single Write Multiple Read) modeled on ATAC [32].

Due to the configurability and regularity of the ONIs, different static wavelength assignment schemes can be used in the network, e.g., source-based wavelength assignment [11], destination-based wavelength assignment [11], and communication-based wavelength assignment [29]. The configuration of ONIs can be defined at either design-time or run-time.

However, different wavelengths can interfere with each other, due to the imperfect coupling in silicon photonic devices. Consequently, the OSNR of an expected signal is reduced after the transmission from the source to the destination, and the corresponding reliability is brought down. In the considered architecture, the laser output power is able to be controlled separately at local ONIs [30], according to the reliability requirement at the destination. This would contribute to the improvement of the laser power efficiency.

IV. RELIABILITY-AWARE JOINT DESIGN METHOD

In this section, we first analyze the influence on the communication reliability of managing application mapping and wavelength assignment separately. Then, an overview of the proposed reliability-aware method is presented. Afterwards, the application mapping and the wavelength assignment are introduced in detail.

A. INFLUENCE ON THE RELIABILITY OF MANAGING APPLICATION MAPPING AND WAVELENGTH ASSIGNMENT SEPARATELY

The result of application mapping has an influence on the received signal power and crosstalk at the studied node, thus resulting in an impact on the communication reliability. The

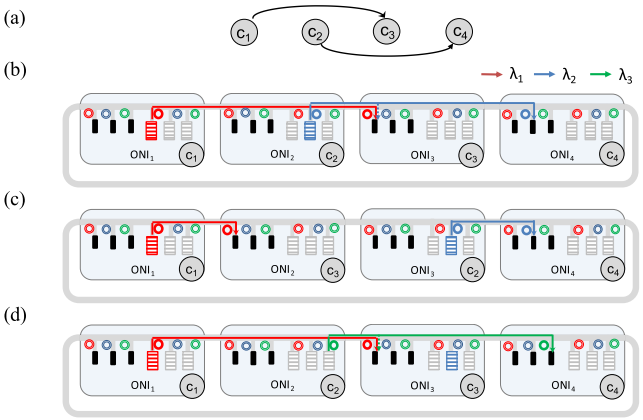

FIGURE 3. The instance of managing application mapping and wavelength assignment separately: a) an example of application core graph; b) an example of mapping result; c) a different mapping result for less crosstalk compared with the case of b); d) the same mapping result but different wavelength assignments for less crosstalk compared with the case of b).

locations of communications in a many-core processor are determined by the result of application mapping. It indicates different lengths of the routing path in one communication and different relative positions of all the communications. Meanwhile, the crosstalk is related to the routing paths of communications and wavelengths assigned to the communications [33].

For instance, the application core graph (in Figure 3-a) with four task cores includes two communications, i.e., $c_1 \rightarrow c_3$ and $c_2 \rightarrow c_4$. One example of application mapped to a network architecture (with four ONIs in ring topology) is shown in Figure 3-b. The communications $c_1 \rightarrow c_3$ and $c_2 \rightarrow c_4$ are mapped onto ONI$_1$ $\rightarrow$ONI$_3$ and ONI$_2$ $\rightarrow$ONI$_4$ respectively, with the communication wavelengths λ_1 (in red) and λ_2 (in blue). Due to the unwanted coupling of wavelength λ_2 along their overlapping path, the crosstalk to the communication $c_1 \rightarrow c_3$ is induced by the communication $c_2 \rightarrow c_4$.

However, the crosstalk is likely to be avoided when the result of application mapping is different. For instance, if the communications $c_1 \rightarrow c_3$ and $c_2 \rightarrow c_4$ are respectively mapped to ONI$_1$ $\rightarrow$ONI$_2$ and ONI$_3$ $\rightarrow$ONI$_4$ (in Figure 3-c), with the same wavelength assignment as Figure 3-b. There is no overlapping path between these two communications, leading to no crosstalk and higher reliability for communication $c_1 \rightarrow c_3$. The "overlapping" here refers to the simultaneous overlap both in space and in time. For instance, two communication pairs communicate with each other at different wavelengths along the same waveguide at the same time. In this case, we consider the two communication pairs to be "overlapping". Our work is based on the worst case, on the assumption that all communication pairs can be executed simultaneously. As for the "temporal" feature when applying our method, this is what we are to consider in the future work with the evaluation under run-time application.

In addition, the crosstalk is also possible to be reduced by applying different wavelength assignments. For instance,

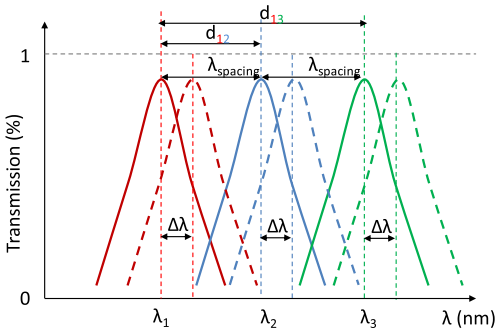

FIGURE 4. The distribution of the available communication wavelengths in Figure 3, i.e., λ_1, λ_2, and λ_3. $\Delta\lambda$ and $\lambda_{spacing}$ indicate the MR wavelength shift between ON and OFF states, and the wavelength spacing between two adjacent wavelengths.

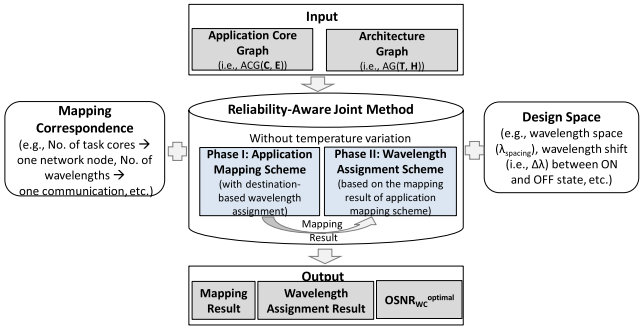

FIGURE 5. Overview of the proposed reliability-aware joint method.

the wavelength λ_3 (in green) is employed for the communication $c_2 \rightarrow c_4$ in Figure 3-d, under the same mapping result with Figure 3-b. The transmission at three wavelengths is shown in details in Figure 4. In two cases of Figure 3-b and Figure 3-d, both the signals at λ_2 and λ_3 would be partially coupled into the MR at λ_1 and induce the crosstalk to the target signal at λ_1. The distance between λ_2 (and λ_3) and λ_1 is denoted as d_{12} (and d_{13}). The crosstalk increases as the wavelength distance decreases, that is, the crosstalk induced by λ_2 is bigger than λ_3. Thus, compared to the case in Figure 3-b, the crosstalk (to the same communication $c_1 \rightarrow c_3$) decreases since the coupling of the wavelength λ_3 is much less due to a bigger distance between λ_1 and λ_3 (as shown in Figure 4), compared to that of the wavelength λ_2. Moreover, the crosstalk is also related to the number of used wavelengths for a given FSR (free spectral range). That is, if there are more available wavelengths for a given FSR, the spacing between two adjacent wavelengths (e.g., $\lambda_{spacing}$) would be smaller. And in this case, the crosstalk induced by other wavelengths to a targeted signal would be higher since the wavelength distance is smaller. Thus, to design a suitable wavelength assignment scheme for the communication (based on an optimal mapping result) is able to further decrease the crosstalk, and thus improve the communication reliability.

Therefore, different results of application mapping and wavelength assignment have different influences on the communication reliability, of which the worst-case OSNR (i.e., $OSNR_{WC}$) is to be taken as the evaluation metric. Under a given network architecture and application graph, to obtain the optimal mapping result, the searching space of mapping solutions increases with order of magnitude as the network scale augments, especially when considering the wavelength assignment at the same time. When the number of network nodes is N, there are N! possible mapping results. For instance, the searching space is as large as 12! ($\approx 4.79 \times 10^8$) for mapping only 12 task cores in one-to-one way. This mapping problem is already proven to NP-hard [20], [34]. To get the optimal result with the traversal search, it is time-consuming and resource-hungry. The intelligent heuristic algorithms are a type of random search method that simulates the evolution of natural organisms or social group behaviors. Through the methods based on intuitive or empirical construction, they can provide some higher quality solutions under the reasonable computing resource conditions (such as computing time and space). Therefore, it is very suitable to use intelligent heuristic algorithms to solve the complex problems such as application mapping or wavelength assignment. The ant colony optimization (ACO) algorithm [35], [36] is one of the widely used intelligent solving algorithms. We utilize this algorithm only as a demonstrative example of solving tools. Based on our proposed method, other optimization algorithms such as genetic algorithm (GA) can also be used for the problem solving. The differences mainly include the parameter design rules and the implementation time of the algorithm.

The number of available wavelengths also has a direct influence on the size of the solution space. The bigger the number of available wavelengths, the larger the problem scale is. With larger problem scale, the designed algorithm can still solve the problem, but the required time of the solving process may become long. In the meanwhile, the solution space of the problem increases factorially. For a larger solution space, the time required to search for a higher-quality solution would also increase. Compared to the precise and exhaustive search method, the heuristic algorithm is able to greatly reduce the consumption of computing resources and time. It is similar regarding the number of increasing mapping nodes.

Thus, a reliability-aware joint method is proposed in our work, in order to deal with this NP-hard problem. The method is focused on the joint consideration of application mapping and wavelength assignment, since these two aspects are co-related with each other in the WDM-based silicon photonic interconnects on chip. We are aware that the temperature variation would lead to an influence on the reliability, which would be explored in the future work.

B. OVERVIEW OF THE PROPOSED RELIABILITY-AWARE JOINT METHOD

In the proposed joint method (as shown in Figure 5), two aspects, i.e., application mapping and wavelength assignment, are considered. The network architecture and

application core graph are taken as the inputs. As for the evaluation of communication reliability, the optimal $OSNR_{WC}$ (i.e., $OSNR_{WC}^{optimal}$) of all the communications is chosen as the metric.

Given the input of the proposed reliability-aware method, a specific application is first mapped onto the network architecture by using our proposed application mapping scheme (i.e., Phase I). Based on the mapping result of Phase I, we propose a reliability-aware wavelength assignment scheme (i.e., Phase II), assigning wavelengths based on communication pairs. At the Phase I, there is a need of certain wavelength assignment before our proposed assignment scheme (i.e., Phase II). So, destination-based wavelength assignment is applied at Phase I, since it can contribute a better result at the stage of application mapping. At the Phase II, our wavelength assignment scheme is proposed and performed based on the application mapping result in Phase I.

Finally, the results of application mapping and wavelength assignment with the $OSNR_{WC}^{optimal}$ are output under the constraint of the mapping correspondence. The design space can be explored as well. The proposed joint method of application mapping and wavelength assignment can be implemented based on various optimization algorithms, corresponding to their characteristics. One heuristic algorithm, i.e., Ant Colony Optimization (ACO) algorithm, is used for the illustration of the proposed method. The ACO algorithm obtains the optimal result through the accumulation and renewal of pheromone along the path after a limited number of iterations, in consideration of the feedback information [35], [36]. It has capability of distributive, parallel, and global convergence. In the process of applying this algorithm, only some characteristics of the specific problem are added to the algorithm's parameter design, in order to make the search proceed in the direction of problem solving. For instance, we take account of the objective function value in the pheromone update process, so that the result with a better objective value can leave more pheromone. Through such iterative search, the result with a better objective value can be screened out. However, at the beginning of iterations, the accumulation of pheromone costs a long time due to the lack of information, which results in a slow solving speed.

The related definitions of input information are shown as follows:

Definition 1 (Application Core Graph): is defined as ACG($\mathbf{C}$, $\mathbf{E}$), where each vertex $c_i \in \mathbf{C}$ represents an task core and each directional edge $e_{ij} \in \mathbf{E}$ represents the communication from task core c_i to task core c_j. The total number of vertexes is assumed to be V in the application core graph, and i and j are in the range of [1, V].

Definition 2 (Architecture Graph): is defined as AG($\mathbf{T}$, $\mathbf{H}$), giving how N network nodes are connected with each other in the physical network layout. The elements $t_i \in \mathbf{T}$ and $h_{ij} \in \mathbf{H}$ ($i \in [1, N]$, $j \in [1, N]$) represent the i^{th} network node and the physical link connecting the network nodes t_i and t_j, respectively.

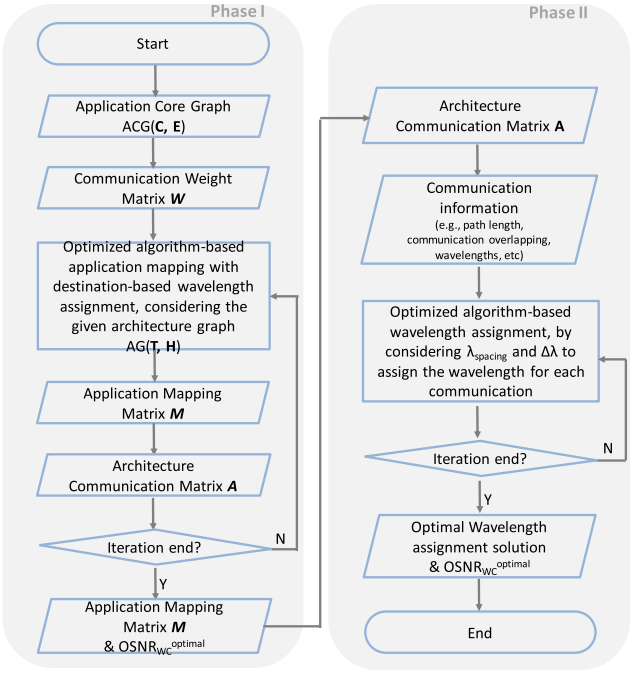

FIGURE 6. The main procedure of the proposed method, with Phase I (i.e., application mapping scheme) and Phase II (i.e., wavelength assignment scheme).

V. RELIABILITY-AWARE APPLICATION MAPPING SCHEME

A. OVERVIEW OF THE OPTIMIZATION ALGORITHM-BASED SCHEME

In the proposed method, a reliability-aware application mapping scheme is firstly designed, of which the main procedure is illustrated in Phase I of Figure 6. The communication weight matrix $\boldsymbol{W}$ is obtained from ACG($\mathbf{C}$, $\mathbf{E}$), indicating the existing communications and communication relationships. By taking consideration of the target architecture represented as AG($\mathbf{T}$, $\mathbf{H}$), the optimization algorithm-based application mapping is implemented with the destination-based wavelength assignment. The optimal result of application mapping can be determined by searching for an application mapping matrix $\boldsymbol{M}$, which enables the architecture communication matrix $\boldsymbol{A}$ corresponding to an optimal objective. The reliability can be improved by the optimization algorithm-based application mapping, during the iterative process of mapping the task cores onto the network nodes in a certain physical layout. The detailed definition is shown as follows.

Definition 3 (Communication Weight Matrix): is defined as $\boldsymbol{W} = (w_{ij})_{V \times V}$, where the element w_{ij} indicates the volume of communication from task core c_i to task core c_j. Here, i and j are in the range of [1, V], and c_i and c_j belong to $\mathbf{C}$ in a given application core graph ACG($\mathbf{C}$, $\mathbf{E}$).

Definition 4 (Application Mapping Matrix): is defined as $\boldsymbol{M} = (m_{ij})_{N \times N}$, where the element m_{ij} indicates the mapping result of a given task core $c_i \in \mathbf{C}$ in ACG($\mathbf{C}$, $\mathbf{E}$) onto a network node $t_j \in \mathbf{T}$ in AG($\mathbf{T}$, $\mathbf{H}$). $\boldsymbol{M}$ is a permutation matrix, and the

value of m_{ij} is 1 when task core c_i is mapped to the network node t_j. Otherwise, m_{ij} is 0.

Definition 5 (Architecture Communication Matrix): is defined as $\boldsymbol{A} = (a_{ij})_{N\times N}$, where the element a_{ij} represents the communication weight of the network nodes t_i to t_j in the architecture after application mapping is applied. It can be obtained based on Communication Weight Matrix $\boldsymbol{W}$ and Application Mapping Matrix $\boldsymbol{M}$, as shown in equation (1).

$$\boldsymbol{A} = \boldsymbol{M}^{\mathrm{T}} \cdot \boldsymbol{W} \cdot \boldsymbol{M} \tag{1}$$

The mapping correspondence (in Figure 5), i.e., the rule of application mapping, is set as follows: i) each task core can be mapped to a network node; ii) two task cores are avoided to be mapped to a same network node. This correspondence is represented by equations (2), (3), (4), and (5).

$$\forall c, \sum_{c\in\boldsymbol{C}} \sum_{t\in\boldsymbol{T}} \sum_{t'\in\boldsymbol{T}, t'\neq t} m_{ct} m_{ct'} = 0 \tag{2}$$

$$\forall t, \sum_{t\in\boldsymbol{T}} \sum_{c\in\boldsymbol{C}} \sum_{c'\in\boldsymbol{C}, c'\neq c} m_{ct} m_{c't} = 0 \tag{3}$$

$$N - \sum_{c\in\boldsymbol{C}} \sum_{t\in\boldsymbol{T}} m_{ct} \geq 0 \tag{4}$$

$$\sum_{c\in\boldsymbol{C}} \sum_{t\in\boldsymbol{T}} m_{ct} - V = 0 \tag{5}$$

In the proposed method, $\mathrm{OSNR_{WC}}$ after mapping is set to be the optimization objective, defined as equation (6). That is, a minimum OSNR exists for the communications in $\boldsymbol{A}$ after each iteration, and the objective is to maximize this minimum OSNR.

$$OSNR_{\mathrm{WC}}^{\mathrm{optimal}} = \mathrm{maximize}\{[OSNR(\boldsymbol{A})]_{\mathrm{minimum}}\} \tag{6}$$

B. SCHEME BASED ON ANT COLONY OPTIMIZATION (ACO) ALGORITHM

The application mapping scheme can be implemented with different optimization algorithms. In this section, the mapping scheme based on ACO algorithm is illustrated. M ants are used to place all the task cores in the application core graph to the nodes in the network architecture during each iteration. After one iteration, only the ant which finds an optimal solution is to leave pheromone along the path being searched, to inspire the next iteration of the searching. Then the pheromone is updated before the next iteration. The placement of task core to network node is defined as a path between the ant colony and a food source. The path is evaluated according to the metric of the corresponding $\mathrm{OSNR_{WC}}$ after application mapping. The max-min ACO algorithm [34] is adopted to avoid collapsing into a local optimal solution, which is caused by excessive accumulation or missing of pheromones. The detailed process is shown as the pseudo code of Algorithm 1 (in Figure 7), with the parameters defined in Table 2.

Each ant is characterized as follows: i) it executes a task independently, and only the ant which finds an optimal value of the objective leaves a pheromone along the path after each iteration; ii) the probability (i.e., p) of an ant to choose a network node for placing an task core depends on the pheromone along the path (i.e., τ) and the heuristic information of the node (i.e., η); iii) ants follow the mapping rule that only one task core can be placed onto a network node, and this restriction is ensured with a tabu list in the algorithm. The related parameters are defined and updated as follows, under the given ACG(**C**, **E**) and AG(**T**, **H**).

Algorithm 1: Application mapping scheme based on ACO

Input: ACG(**C**, **E**), AG(**T**, **H**)
Output: mapping solution, $OSNR_{WC}^{optimal}$
/***Initialization***/
Set parameters value M, α, β, ρ, Q
Initialize all the pheromone values to τ_0

/***nth Iteration***/
for ant m from 1 to M **do**
  for i from 1 to V **do**
    Generate a Tabu-search table $\boldsymbol{T_{used,i}^{m}(n)} = \emptyset$
    Generate the allowed node set $\boldsymbol{T_{available,i}^{m}(n)}$
    Calculate expected heuristic information according to eq.(8)
    for j from 1 to N **do**
      Calculate probability $p_{ij}^{m}(n)$ according to eq.(6)
      P_j= Sum($p_{ik}^{m}(n)$), where $k\in[1, j]$
    end for
    /***Roulette selection***/
    Generate a random number NUM, where $NUM\in(0,1)$
    if $NUM < P_j$ **then**
      Select node t_j to place core c_i, where $t_j\in\mathbf{T}$, $c_i\in\mathbf{C}$
      Move the assigned node t_j to $\boldsymbol{T_{used,i}^{m}(n)}$
    end if
  end for
  Calculate the objective value (i.e., $OSNR_{WC}$) for ant m
end for
Store the best solution
Update pheromone information $\tau_{ij}(n)$ according to eq.(11) for nth iteration

/***Iteration end***/
Return the best result after all the iteration, including the corresponding mapping solution and $OSNR_{WC}^{optimal}$

FIGURE 7. Pseudo-code of application mapping scheme based on ACO.

TABLE 2. Parameters in the ACO algorithm.

Parameter	Definition
M	The number of ants
V	The number of task cores in the ACG(**C**,**E**)
N	The number of network nodes
$OSNR_{WC}^{optimal}$	The worst-case $OSNR$ corresponding to the optimal solution in the mapping scheme
τ_0	Initialized pheromone
α	Heuristic factor of information ($\alpha\in[1, 2]$)
β	Expected heuristic factor ($\beta\in[2, 6]$)
ρ	Evaporation coefficient of information ($\rho\in[0, 1]$)
$\tau_{ij}(n)$	Pheromone when mapping c_i to t_j at the nth iteration
$\Delta\tau_{ij}^{max}$	Pheromone increment that the ant with $OSNR_{WC}^{optimal}$ leaves
$\eta_{ij}(n)$	Heuristic information when mapping c_i to t_j at the nth iteration
Q	Pheromone intensity (a positive constant value)
K	A positive constant different from Q (K>$OSNR$)

1) ANT COLONY INITIALIZATION

In the first iteration, the ant colony is initialized, and there is no inspiration pheromone along the paths. The pheromone is initialized as τ_0 along each path, and the selection probability of each task core is set to be the same.

2) CALCULATION OF SELECTION PROBABILITY

In the process of finding a solution, ants select the network node to place the task core through a random mechanism. For

the ant m ($m \in [1, M]$) at the n^{th} iteration, the probability of placing the task core c_i to the network node t_j can be calculated as follows:

$$p_{ij}^{m}(n) = \begin{cases} \dfrac{[\tau_{ij}(n)]^{\alpha}[\eta_{ij}(n)]^{\beta}}{\sum_{t_k \in \boldsymbol{T}_{\boldsymbol{available},\boldsymbol{i}}^{\boldsymbol{m}}(\boldsymbol{n})} [\tau_{ik}(n)]^{\alpha}[\eta_{ik}(n)]^{\beta}}, \\ \qquad t_j \in \boldsymbol{T}_{\boldsymbol{available},\boldsymbol{i}}^{\boldsymbol{m}}(\boldsymbol{n}) \\ 0, \qquad else \end{cases} \tag{7}$$

Here, parameters α and β determine the relative importance of the pheromone $\tau_{ij}(n)$ versus the heuristic information $\eta_{ij}(n)$. The selected nodes belong to the set $\boldsymbol{T}_{\boldsymbol{available},\boldsymbol{i}}^{\boldsymbol{m}}(\boldsymbol{n})$, calculated by the following equation.

$$\boldsymbol{T}_{\boldsymbol{available},\boldsymbol{i}}^{\boldsymbol{m}}(\boldsymbol{n}) = \boldsymbol{T} - \boldsymbol{T}_{\boldsymbol{used},\boldsymbol{i}}^{\boldsymbol{m}}(\boldsymbol{n}), \tag{8}$$

where $\boldsymbol{T}_{\boldsymbol{used},\boldsymbol{i}}^{\boldsymbol{m}}(\boldsymbol{n})$ represents the set of the already mapped nodes for the previous cores (i.e., c_1, c_2, …, c_{i-1}) with the ant m at the n^{th} iteration, and it is empty when i equals to 1. Based on the selection probability in equation (7), the bigger the pheromone (i.e., $\tau_{ij}(n)$) and the heuristic information (i.e., $\eta_{ij}(n)$) are, the higher the probability of placing task core c_i to network node t_j is.

According to communication characteristics of a specific application, the heuristic information $\eta_{ij}(n)$ of mapping the task core c_i to the network node t_j can be defined as:

$$\eta_{ij}(n) = \frac{\sum_{t_k \in \boldsymbol{T}_{\boldsymbol{used},\boldsymbol{i}}^{\boldsymbol{m}}(\boldsymbol{n})} d(j,k)}{\sum_{t_r \in \boldsymbol{T}_{\boldsymbol{available},\boldsymbol{i}}^{\boldsymbol{m}}(\boldsymbol{n}), t_k \in \boldsymbol{T}_{\boldsymbol{used},\boldsymbol{i}}^{\boldsymbol{m}}(\boldsymbol{n})} d(r,k)}, \quad t_j \in \boldsymbol{T}_{\boldsymbol{available},\boldsymbol{i}}^{\boldsymbol{m}}(\boldsymbol{n}) \tag{9}$$

Here, $d(j,k)$ is determined by whether there is communication requirement between node t_j (mapped by the core c_i) and the previously placed node t_k (mapped by the core $c_x \in [c_1, c_2, \ldots, c_{i-1}]$), indicating the correlation of two nodes. Its value can be calculated as follows:

$$d(j,k) = \begin{cases} 1, & w/o\ communication\ between\ t_j\ and t_k \\ 1+d_{jk}, & w/\ \ communication\ between\ t_j\ and\ t_k \end{cases} \tag{10}$$

And d_{jk} is detailed as:

$$d_{jk} = \begin{cases} |j-k|, & or \begin{array}{l} communication\ t_j \rightarrow t_k\ exists \& j<k \\ communication\ t_j \leftarrow t_k\ exists\ \&\ j>k \end{array} \\ N-|j-k|, & or \begin{array}{l} communication\ t_j \rightarrow t_k\ exists \& j>k \\ communication\ t_j \leftarrow t_k\ exists\ \&\ j<k \end{array} \end{cases} \tag{11}$$

3) UPDATE OF PHEROMONE

To enhance the characteristic of superior solutions, the pheromone along the path is updated after each iteration, by increasing and decreasing the pheromone of superior and inferior solutions, respectively. The pheromone $\tau_{ij}(n)$ is updated according to the following rules.

$$\tau_{ij}(n+1) = (1-\rho) \cdot \tau_{ij}(n) + \Delta\tau_{ij}^{max}(n) \tag{12}$$

$$\Delta\tau_{ij}^{\max}(n) = \begin{cases} \dfrac{Q}{K - OSNR_{WC}} & if\ core\ c_i\ is\ mapped\ to\ node\ t_j \\ 0 & otherwise \end{cases} \tag{13}$$

However, if the pheromone $\tau_{ij}(n+1)$ is smaller than the lower limit τ_{min} or bigger than the upper limit τ_{max}, it is set to be the corresponding boundary value, i.e., τ_{min} or τ_{max}.

VI. RELIABILITY-AWARE WAVELENGTH ASSIGNMENT SCHEME

After obtaining the result of application mapping, a reliability-aware wavelength assignment scheme is proposed, employing the optimization algorithm, to further reduce the influence of crosstalk on the communication reliability. By taking into consideration of the distance of wavelengths assigned for the overlapping communications, the proposed wavelength assignment scheme can reduce the unwanted coupling in comparison with the traditional (static) schemes, e.g., source-based, destination-based, and communication-based wavelength assignment schemes. In this section, the proposed wavelength assignment scheme is first introduced, then the traditional wavelength assignment schemes are studied in detail.

A. THE PROPOSED SCHEME

In the proposed wavelength assignment scheme, the heuristic algorithms are applied to assign proper wavelengths for the communication paths, especially for the ones with overlapping. For the assignment, the ''overlapping'' in both space and time are considered simultaneously. Different communications can happen at the same time with the same wavelength if there is no spatial or temporal overlap between or among certain communications. Our work is based on the worst case, on the assumption that all communication pairs can be executed simultaneously. As a result, the proposed wavelength assignment scheme can minimize both the crosstalk suffered by the studied communication path and the crosstalk induced by the studied communication path to other paths. The main procedure of the proposed reliability-aware wavelength assignment is shown in the Phase II of Figure 6, of which the pseudo code is illustrated in Figure 8.

Based on the architecture communication matrix $\boldsymbol{A}$, communication information, e.g., the lengths and overlapping relationship of communication paths, can be obtained. The communication paths are firstly ranked according to their lengths, e.g., from the longest to the shortest, and stored in the path set $\boldsymbol{Path} = \{path_1, path_2, \ldots, path_j, \ldots, path_{Npath}\}$. The wavelengths that are available for communication are marked as a set $\boldsymbol{WL_{available}} = \{\lambda_1, \lambda_2, \ldots, \lambda_i, \ldots, \lambda_{NWL}\}$, where N_{WL} indicates the total number of available wavelengths. Given the available wavelength range WL_{range}, the wavelength λ_i is obtained by $\lambda_i = \lambda_1 + \lambda_{spacing} \times (i\text{-}1)$, where the wavelength spacing $\lambda_{spacing}$ can be calculated by (WL_{range}/N_{WL}). The wavelengths (in nm) in $\boldsymbol{WL_{available}}$ are assigned to communications by considering

Algorithm 2: **Wavelength Assignment scheme based on ACO**

Input: architecture communication matrix $\boldsymbol{A}$
Output: wavelength assignment result
/***Initialization***/
Set parameters value M, α, β, ρ, Q
Initialize all the pheromone values to τ_0

/***nth Iteration***/
for ant m from 1 to M **do**
  for i from 1 to N_{WL} **do**
    Generate a Tabu-search table $\boldsymbol{Path_{used,i}^{m}(n)}= \emptyset$
    Generate the allowed path set $\boldsymbol{Path_{available,i}^{m}(n)}$
    Calculate heuristic information according to adapted eq.(9)
    for j from 1 to N_{path} **do**
      Calculate probability $p_{ij}^{m}(n)$ according to adapted eq. (7)
      P_j= Sum($p_{ik}^{m}(n)$), where $k \in [1, j]$
    end for
    /***Roulette selection***/
    Generate a random number NUM, where $NUM \in (0,1)$
    if $NUM < P_j$ **then**
      Select the $path_j$ to assign the wavelength λ_i, where $path_j \in \boldsymbol{Path}$, $\lambda_i \in \boldsymbol{WL_{available}}$
      Move the assigned $path_j$ to $\boldsymbol{Path_{used,i}^{m}(n)}$
    end if
  end for
  Calculate the objective value (i.e., $OSNR_{WC}$) for ant m
end for
Store the best wavelength assignment solution
Update pheromone information $\tau_{ij}(n)$ according to adapted eq.(12) for nth iteration

/***Iteration end***/
Return the best result after all the iteration, including the corresponding wavelength assignment result and $OSNR_{WC}^{optimal}$

FIGURE 8. Pseudo-code of wavelength assignment scheme based on ACO.

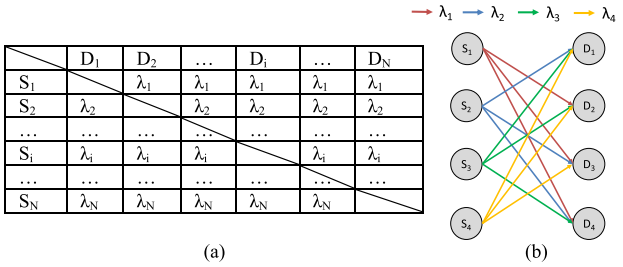

FIGURE 9. Source-based wavelength assignment scheme: a) the detailed rules; b) the assignment result of 4 network nodes.

$OSNR_{WC}$. The process is iterated until achieving the wavelength assignment results which lead to the optimal $OSNR_{WC}$ (i.e., $OSNR_{WC}^{optimal}$). In the wavelength assignment scheme, the wavelength resources (e.g., λ_i) and the to-be-assigned paths (e.g., $path_j$) respectively correspond to the task cores (e.g., c_i) and the to-be-mapped network nodes (e.g., t_j) from the aspect of the algorithm. More detailed peocess can be referred to [37]. Note that only one-to-one assignment is considered, i.e., one wavelength for one communication.

B. THE TRADITIONAL SCHEMES

To decrease the crosstalk, different wavelength assignment schemes are studied in this work: i) source-based wavelength assignment [11] (in Figure 9), in the manner of Single-Write-Multiple-Read (SWMR); ii) destination-based wavelength assignment [11] (in Figure 10), in the manner of

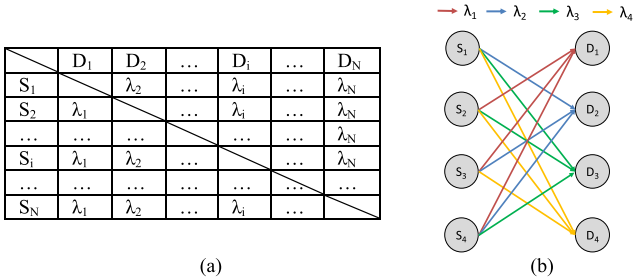

FIGURE 10. Destination-based wavelength assignment scheme: a) the detailed rules; b) the assignment result of 4 network nodes.

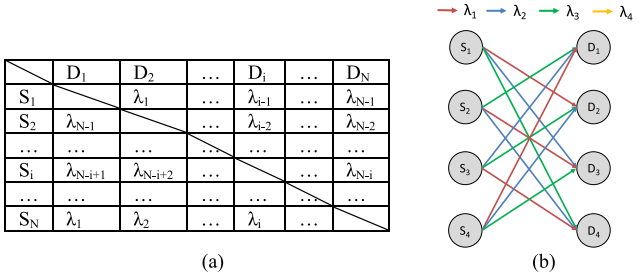

FIGURE 11. Communication-based wavelength assignment scheme: a) the detailed rules; b) the assignment result of 4 network nodes.

TABLE 3. The parameters of the photonic interconnects on chip [33].

Symbol	Parameter	Value
l_p	Propagation loss	-0.274dB/cm
l_b	Bending loss	0.005dB
λ_0	Initial wavelength of the considered range	1550 nm
FSR	Free Spectrum Range, i.e., wavelength range	59 nm
$\Delta\lambda$	Wavelength drift between ON and OFF states	0.16nm

Multiple-Write-Single-Read (MWSR); iii) communication-based wavelength assignment [29] (in Figure 11), in the manner of Multiple-Write-Multiple-Read (MWMR).

For the source-based wavelength assignment scheme, the communication wavelength λ_i used for any destination D_j ($\forall j \in [1, N]$) is assigned according to the ID of the source node S_i. That is to say, the communications from the same source but to different destinations adopt the same wavelength λ_i, depending on the source's ID i. For instance, the source node S_1 transmits data to different destination nodes (e.g., D_1, D_2, D_3, and D_4) by using the same wavelength of λ_1, as shown in Figure 9.

For the destination-based wavelength assignment scheme, the communication wavelength used for any source node S_i ($\forall i \in [1, N]$) is assigned according to the ID of destination node D_j. That is to say, the communications from different source nodes but to the same destination node adopt the same wavelength λ_j, depending on the destination's ID j. For instance, the source node S_1 transmits data to different destination nodes (e.g., D_1, D_2, D_3, and D_4) by using different wavelengths, i.e., λ_1, λ_2, λ_3, and λ_4, as shown in Figure 10.

For the communication-based wavelength assignment, on one hand, the wavelengths can be assigned simply in a

regular way. For instance, Figure 11 demonstrates an example of communication-based wavelength assignment scheme with the Latin Square [38]. Similarly, the wavelengths can be assigned to communication paths in an ordinal order (i.e., C-based (O) for short), inverse order (i.e., C-based (I) for short), and random order (i.e., C-based (R) for short). For instance, communication paths are labelled as $\{path_1, path_2, \ldots, path_N\}$, which are extracted from the communication weight matrix $\boldsymbol{W}$. Then, the wavelength assignment result is $\{\lambda_1, \lambda_2, \ldots, \lambda_N\}$ in the ordinal order, and $\{\lambda_N, \lambda_{N-1}, \ldots, \lambda_1\}$ in the reverse order, corresponding to the IDs of communication paths. On the other hand, communication wavelengths can be assigned more flexibly. A reliability-aware scheme is used in this work, and the wavelengths are assigned according to the communication requirement and potential crosstalk, in order to reduce the influence of the crosstalk on the communication reliability.

VII. ANALYTICAL OSNR MODEL

This section presents the analytical OSNR model used in the proposed method to evaluate the communication reliability. Based on OSNR, BER (bit error rate) can be modeled and calculated [17]. The optical signal inevitably suffers insertion losses along the whole communication path from the source to the destination node, and experiences optical crosstalk from other different wavelengths at the same time if there are overlapping communications passing by the destination. The factors in network level determining the reliability are: network scale, network topology, the architecture of optical network interface, and the number of wavelengths.

A generic architecture with N_{ONI} interfaces is used as the illustrative example, and N_{WL} wavelengths are applied to emit and receive the optical signals, as shown in Figure 12. N_{WL} lasers and N_{WL} receivers, each at a specific wavelength, are employed to inject and eject optical signals in each interface respectively.

In the OSNR model, the optical signal at the wavelength λ_j transmitting from the source node ONI_s to the destination node ONI_d is analytically evaluated. The expected signal power at the destination node $OP_{signal}[j]$ is calculated as follows:

$$OP_{signal}[j] = OP_{in,s,j} \cdot L_{waveguide} \cdot \varphi_{t,signal}^{total} \cdot [\varphi_d(\lambda_j, \lambda_j)]^2 \quad (14)$$

where $OP_{in,s,j}$ is the input signal power of ONI_s at the wavelength λ_j. $L_{waveguide}$ indicates the signal losses induced by the waveguide along the communication path, and it consists of the propagation loss and bending loss. $\varphi_{t,signal}^{total}$ represents the signal transmission efficiency at the through port of MRs along the communication path, and $\varphi_d(\lambda_j, \lambda_j)$ represents the signal transmission efficiency at the drop port of MRs in the source and destination nodes [6], [33]. $\varphi_{t,signal}^{total}$ can be calculated as follows:

$$\varphi_{t,signal}^{total} = \prod_{n=1}^{j-1} \varphi_t(\lambda_j, \lambda_n + d_n \cdot \Delta\lambda) \cdot [\prod_{n=1}^{N_{wl}} \varphi_t(\lambda_j, \lambda_n + d_n \cdot \Delta\lambda)]^{l_{s\to d}-1} \quad (15)$$

where $\varphi_t(\lambda_j, \lambda_n + \Delta\lambda)$ represents the signal transmission efficiency at the through port of MR, and λ_n is the resonant wavelength of the MRs encountered along the communication path. $\Delta\lambda$ is the wavelength shift of an MR between its ON and OFF states. d_n, of which the value can be 0 or 1, indicates the state of MR (i.e., ON or OFF) at the resonant wavelength λ_n along the communication path. In the network in Figure 12, when an MR is ON, it is used for detecting optical signal and drops the signal to the photodetector. Otherwise, the MR has no impact on the signal, and the signal passes by the MR and transmits along the waveguide. The parameter $l_{s\to d}$ indicates the distance from the source to the destination of a studied communication. It can be calculated as follows:

$$l_{ONIs\to ONId} = \begin{cases} ONI_d - ONI_s, & when\ ONI_s < ONI_d \\ N_{ONI} - ONI_s + ONI_d, & when\ ONI_s > ONI_d \end{cases} \quad (16)$$

For the expected signal at the wavelength λ_j in the destination interface ONI_d, the crosstalk comes from the other signals at different wavelengths (emitted by the interface ONI_m) passing by the receiver in ONI_d. For instance, the communication $ONI_k \to ONI_{NONI}$ (at wavelength λ_i) in Figure 12 induces crosstalk to the expected signal of communication $ONI_l \to ONI_r$ (at the wavelength λ_j) at the j^{th} receiver in ONI_r. The crosstalk accumulated at the j^{th} receiver in the interface, i.e., $OP_{crosstalk}[j]$, can be calculated as follows:

$$OP_{crosstalk}[j] = \sum_{i\neq j}^{N_{wl}} OP_{crosstalk,i}[j] \quad (17)$$

where $OP_{crosstalk,i}[j]$ indicates the crosstalk induced by the other signal at the wavelength λ_i, and it can be calculated as follows:

$$OP_{crosstalk,i}[j] = OP_{in,m,i} \cdot L_{waveguide} \cdot \varphi_d(\lambda_i, \lambda_i) \cdot \varphi_{t,crosstalk}^{total} \cdot \varphi_d(\lambda_i, \lambda_j) \quad (18)$$

where $OP_{in,m,i}$ is the input power of ONI_m at the wavelength λ_i. $\varphi_{t,crosstalk}^{total}$ represents the crosstalk transmission efficiency at the through port of all MRs along the overlapping communication path. $\varphi_d(\lambda_i, \lambda_j)$ represents the crosstalk transmission efficiency at the drop port of MR in the destination node. $\varphi_{t,crosstalk}^{total}$ can be calculated as follows:

$$\varphi_{t,crosstalk}^{total} = [\prod_{n=1}^{N_{wl}} \varphi_t(\lambda_i, \lambda_n + d_n \cdot \Delta\lambda)]^{l_{m\to d}-1} \cdot \prod_{n=1}^{j-1} \varphi_t(\lambda_i, \lambda_n + d_n \cdot \Delta\lambda) \quad (19)$$

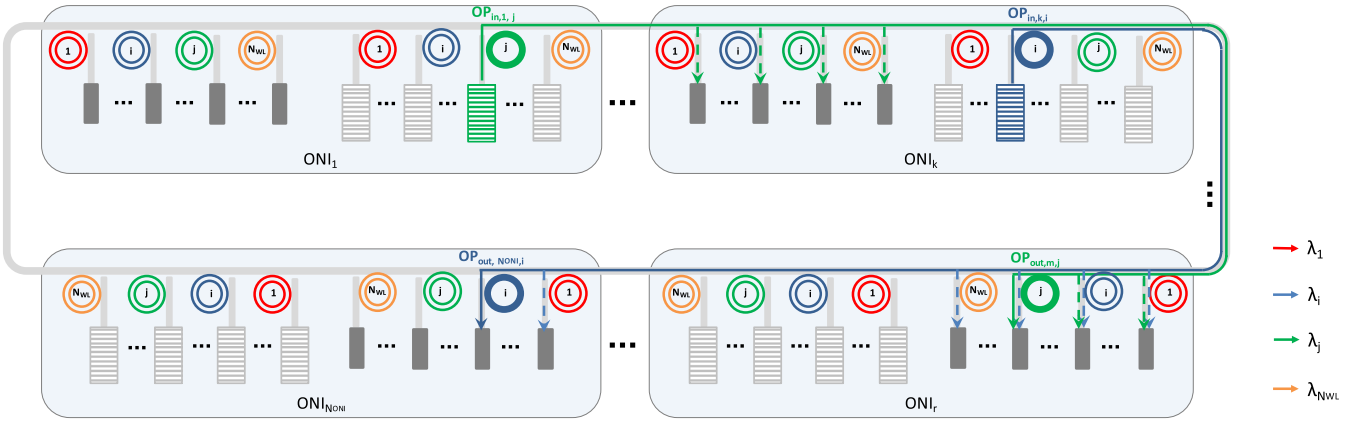

FIGURE 12. Generic architecture for the establishment of the OSNR model.

On this basis, the OSNR model of optical communication from the source node ONI_s to the destination node ONI_d at the wavelength λ_j can be established as follows.

$$OSNR_{s\to d}[j] = 10\lg\frac{OP_{signal}[j]}{OP_{crosstalk}[j]} \tag{20}$$

VIII. EVALUATION RESULTS

The case study for the proposed method is firstly detailed. Then the proposed method is validated and the performance improvement is studied. In the simulations, the proposed method is evaluated respectively under different applications and with different optimization algorithms. The influence of wavelength assignment schemes is analyzed afterwards., and the impact factors, i.e., wavelength spacing and wavelength drifts, are considered as well.

A. CASE STUDY

For the evaluation, a set of typical application benchmarks are considered, e.g., PIP, MWD, 263enc mp3dec, and mp3enc mp3dec [20], [39] respectively in Figure 13-a, -b, -c, and -d. These synthetic models of the real-world application benchmarks are also used in [20], [36], [40], [41], [42] to evaluate proposed strategies, different from the application modeling from high level programs to workload characterization for manycore platform design in [43]–[45]. The application benchmarks are abstracted into application core graphs (i.e., different directed graph), and the communications between various cores. The task core graphs in our evaluation are from [20], [39]. Each vertex in the application core graph represents a task core, and the directed edge represents the communication between cores. The communication volume exchanged between core are denoted by the weight of the edges. Note that the application benchmarks are utilized to evaluate the efficiency of the proposed method, but the method is not limited by the specific applications.

In our work, the network architecture in Figure 2 is used for application mapping, and it is able to assign wavelengths with the three different methods (i.e., source-based, destination-based, and communication-based wavelength assignments) by tuning on/off the corresponding MRs. The case studies are carried out on an Intel Core i5 platform with 3.0GHz clock frequency and 8GB memory space. The parameters related to photonic interconnects are from [33] and listed in Table 3. The number of wavelengths equal to the number of network nodes in the evaluation.

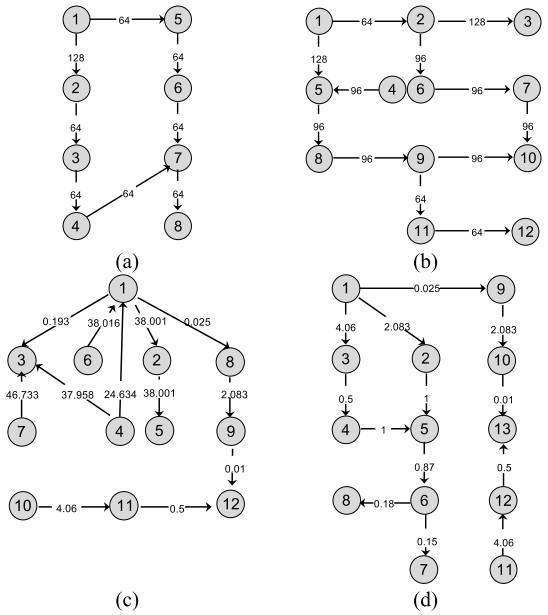

FIGURE 13. Application core graphs of different applications considered in the case study: a) PIP, b) MWD, c) 263enc mp3dec, and d) mp3enc mp3dec [20], [39].

The application core graphs of different applications [20], [39] are shown in Figure 13. The vertexes in grey (i.e., task cores) represent the units which are responsible for the functions. The edges between different vertexes represent the communication between different task cores. The directions of these edges indicate the communication direction. The values along the edges present the communication weight. For instance, in Figure 13-a, the edge from ① to ⑤ represents the

TABLE 4. Communication weight matrix W of the PIP application.

D / S	1	2	3	4	5	6	7	8
1		128	0	0	64	0	0	0
2	0		64	0	0	0	0	0
3	0	0		64	0	0	0	0
4	0	0	0		0	0	64	0
5	0	0	0	0		64	0	0
6	0	0	0	0	0		64	0
7	0	0	0	0	0	0		64
8	0	0	0	0	0	0	0	

TABLE 5. The application mapping matrix M of Figure 1.

No. of task cores \ No. of ONIs	1	2	3	4	5	6	7	8
1		0	0	0	1	0	0	0
2	0		0	0	0	1	0	0
3	0	0		0	0	0	1	0
4	0	0	0		0	0	0	1
5	0	0	1	0		0	0	0
6	0	0	0	1	0		0	0
7	1	0	0	0	0	0		0
8	0	1	0	0	0	0	0	

communication from core 1 to core 5, and the communication weight is 64MB/s [39].

For different applications, the communication weight matrix $\boldsymbol{W}$ can be obtained from the application core graph, in consideration of the communication volume between the source core (''S'' for short) and destination core (''D'' for short). For instance, Table 4 gives the weight matrix of the application PIP, where ''0'' represents no communication exists, and the numbers indicate the volume of the related communications.

The application mapping matrix $\boldsymbol{M}$ is obtained after mapping the application core graph to the network architecture (e.g., in Figure 1). One-to-one mapping is considered in the case study. The wavelength-routing communication is based on different wavelengths. In embedded systems, the process and interdependencies of application tasks in the real world are represented by means of application core graphs [39], and then the task cores are allocated to the available Processing Elements (PEs). In general, we execute the application mapping scheme as long as the number of task cores in the core graph is smaller than or equal to the network size. The resource is utilized more sufficiently when the number of task cores is equal to the number of network nodes, without idle network nodes. If the number of task cores is bigger than the number of network nodes, the task graph needs to be further divided before application mapping. That is to say, multiple tasks need to be allocated to a PE through scheduling process [36]. Different scheduling algorithms have been researched [46]. If the number of task cores is equal to or smaller than the number of network nodes, the application mapping can be performed directly.

In the application mapping matrix of Table 5, ''1'' represents that the corresponding task core is mapped onto the dedicated ONI, and vice versa for ''0''. For instance, ''1'' is for task core 2→ONI 6 in the matrix, which represents that task core 2 is mapped onto the ONI 6.

TABLE 6. The value of parameters in optimization algorithms: a) ACO and b) GA.

(a)

Parameter	Value	Parameter	Value
M, V	N (8 or 12)	ρ	0.5
τ_0	1	Q	60
α	1	K	150
β	5	(τ_{min}, τ_{max})	(0.5, 2)

(b)

Parameter	Definition	Value
V	The number of application task cores	N (8or12)
N_p	The size of population	100
P_c	Crossover probability ($P_c \in [0.4, 0.99]$)	0.55
P_m	Mutation probability ($P_m \in [0.001, 0.1]$)	0.01

The parameters used in the ACO algorithm is shown in Table 6-a. In addition, Genetic algorithm (i.e., GA) [47] is employed for the evaluation, to further show the flexibility of applying other optimization algorithms. GA is usually used to solve the unconstrained and constrained nonlinear optimization problems based on the natural selection process, mimicking the biological evolution. GA iteratively modifies the population consisting of individual solutions. In each step, GA randomly selects individuals from the current population and uses them as a parent to generate the next generation of children. After several generations, the group gradually ''evolves'' into an optimal solution. The related parameters are in Table 6-b.

B. VALIDATION AND PERFORMANCE OF THE PROPOSED METHOD BASED ON ACO

In this subsection, the simulation results are first validated under the destination-based wavelength assignment, with the traversal mapping and random mapping schemes [36], [48]. In the traversal mapping, $\mathrm{OSNR_{WC}}$ is evaluated for each mapping solution, namely $8! = 40320$ mapping solutions are considered. In the random mapping, a given number of solutions are selected randomly.

Figure 14 shows the evaluation results of the $\mathrm{OSNR_{WC}}$ under the application of PIP, with the traversal mapping (Figure 14-a and -b) and random mapping (Figure 14-c and -d). The distributions of $\mathrm{OSNR_{WC}}$ with different mapping schemes are shown in scatter plots in Figure 14-a and -c. The probability distribution which highlights the statistical characteristics in scatter plots are shown in Figure 14-b and -d. According to the traversal mapping, the optimal $\mathrm{OSNR_{WC}}$ is 47.1dB. Based on the scatter plots in Figure 14-a, most of the $\mathrm{OSNR_{WC}}$ values are between 41dB and 44dB, which accounts for about 90% of the results according to Figure 14-b.

From the results, the probability distribution of $\mathrm{OSNR_{WC}}$ with random mapping shows a similar characteristic with the traversal mapping. For instance, $\mathrm{OSNR_{WC}}$ in both mapping schemes reaches around 42dB with the highest probability,

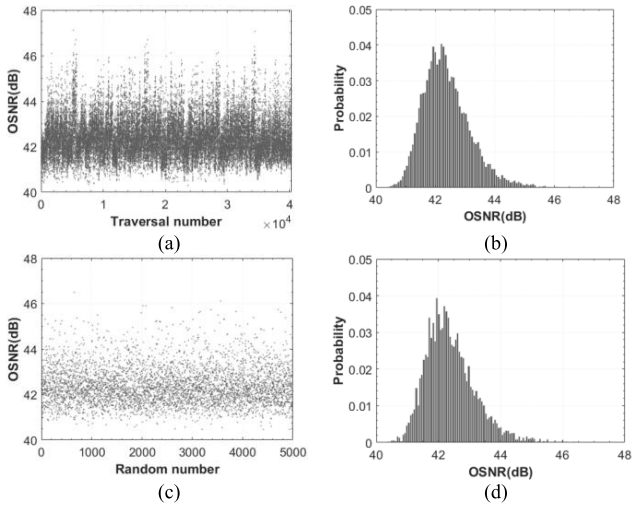

FIGURE 14. The $OSNR_{WC}$ distribution with different mapping schemes under PIP: a) OSNR with traversal mapping in scatter plots; b) probability distribution of OSNR for the total of 40320 mapping solutions; c) OSNR with random mapping under 5000 times in scatter plots; d) probability distribution of OSNR for 5000 mapping solutions.

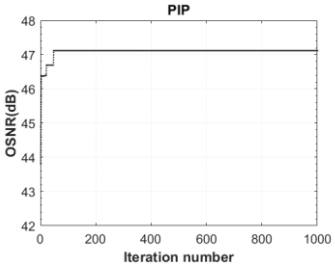

FIGURE 15. $OSNR_{WC}$ evaluated with the proposed application mapping scheme based on ACO algorithm under PIP.

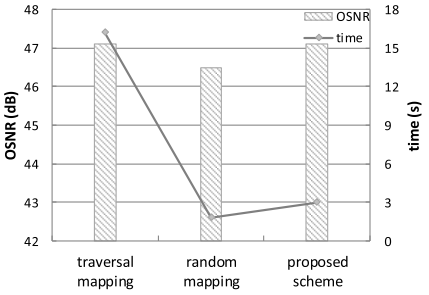

FIGURE 16. The tradeoff between reliability and time consumption with different mapping schemes.

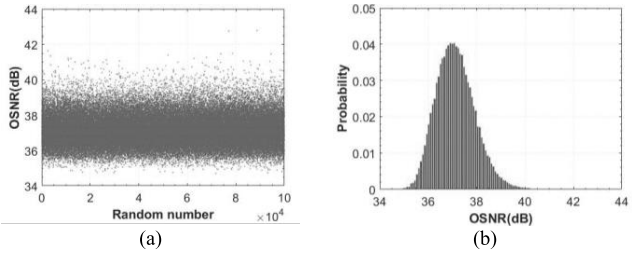

FIGURE 17. $OSNR_{WC}$ results under the application of MWD, with the random mapping, a) distribution of OSNRs under 100,000 times of mapping solutions in scatter plots; b) probability distribution of OSNRs.

according to Figure 14-b and -d. Compared to the traversal mapping, the optimal result with the random mapping can be obtained much faster, with 5000 mapping solutions instead of 40320. And the results with the random mapping are still representative by considering the distribution and statistical characteristic. Therefore, in this work the random mapping is used under the applications, since the traversal mapping requires more time and resources.

The proposed application mapping scheme is implemented based on ACO algorithm, to evaluate the $OSNR_{WC}$ under PIP. Figure 15 presents the results of our proposed method, with the related parameters set as Table 6-a. As the iteration number gets bigger, the $OSNR_{WC}$ increases gradually, and becomes stable at around 47.1dB finally, which equals to the optimal value obtained in traversal mapping in Figure 14.

Figure 16 illustrates the optimal $OSNR_{WC}$ and the consumed time (for obtaining the optimal $OSNR_{WC}$) by utilizing different application mapping schemes, i.e., traversal mapping, random mapping, and the proposed mapping scheme based on ACO. The proposed mapping scheme can achieve a better tradeoff between reliability and time consumption, as shown in Figure 16. For the traversal mapping and the proposed method, their obtained optimal $OSNR_{WC}$ reaches 47.1dB, while it is 46.5dB for the random mapping. However, in the aspect of time consumption, the proposed method only costs 3.0s, while 16.2s and 1.8s for the traversal mapping and random mapping, respectively. To obtain the same $OSNR_{WC}$, the proposed method takes about 81.6% less time than the traversal mapping. In the meanwhile, the search ability of our proposed scheme outperforms the random mapping due to the exploration of potentially optimal solutions.

C. ANALYSIS UNDER DIFFERENT APPLICATIONS BASED ON ACO

Figure 17 shows the evaluation results of random mapping under different applications, with 100,000 mapping solutions generated randomly. The scatter distribution and probability distribution are respectively given in Figure 17-a and -b. Most of the OSNR values fall in the range of 36dB to 38dB, and about 90% of the values are between 35dB and 40dB, below the biggest value of 42.8dB. Meanwhile, the random mapping takes ∼111.5s to obtain the optimal results.

As shown in Figure 18-a, the proposed mapping scheme is evaluated with the same parameters as random mapping under the application of MWD [39]. As the iteration number progresses, the $OSNR_{WC}$ increases and finally reaches an optimal value, i.e., 44.6dB. Moreover, compared to the case in PIP, there are more task cores in MWD to be mapped, with more complicated communication characteristics, as shown in Figure 13. The optical signal might experience a longer communication path with more path overlapping, which induces less signal power and more crosstalk power. As a

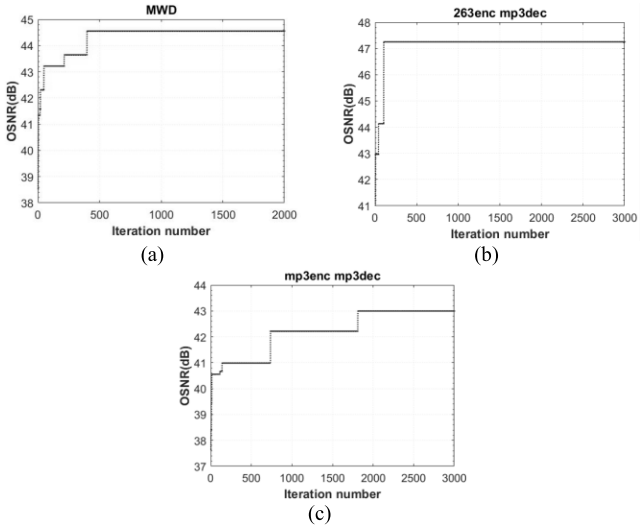

FIGURE 18. $OSNR_{WC}$ results evaluated with the proposed mapping scheme, under different applications: a) MWD, b) 263enc mp3dec, and c) mp3enc mp3dec.

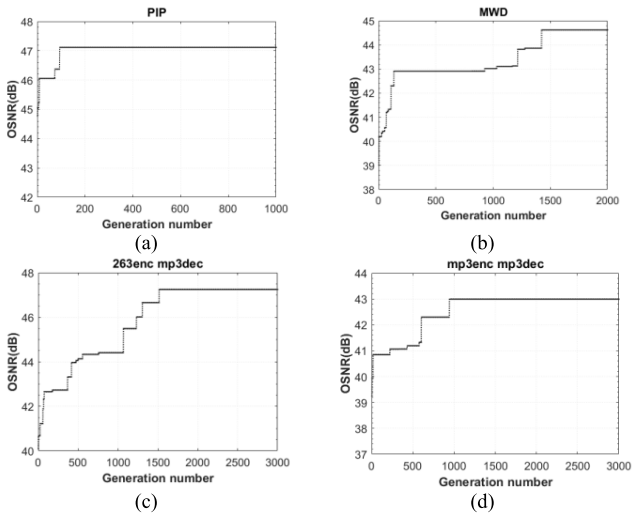

FIGURE 19. $OSNR_{WC}$ results evaluated with the proposed mapping scheme based on GA under different applications: a) PIP; b) MWD; c) 263enc mp3dec; d) mp3enc mp3dec.

result, the optimal $OSNR_{WC}$ under MWD decreases by 2.5dB compared to PIP. In addition, more times of iterations are required to reach the optimal value, due to the existence of more possible mapping solutions. For instance, the $OSNR_{WC}$ result gets stable at about 400 times of iterations under MWD, while at less than 100 times of iterations under PIP. To verify the accuracy of results, 200 rounds of simulations are performed with the same configuration, and it turns out that the optimal $OSNR_{WC}$ almost keeps the same with only ignorable fluctuation. Meanwhile, the proposed scheme takes about 48.4s in average for reaching the optimal value, which is about 50% less than the random mapping.

Similarly, the evaluation results under the applications of 263enc mp3dec and mp3enc mp3dec [39] are given in Figure 18-b and -c, respectively. In consideration of the communication patterns in Figure 13, similar conclusions can be achieved: i) the communication paths indicate less overlapping under 263enc mp3dec, thus the proposed mapping scheme can reach a higher $OSNR_{WC}$ of 47.3dB; ii) there are more task cores in the application core graph, and the communication paths are with more overlapping, thus the proposed mapping scheme gets a lower $OSNR_{WC}$ of 43.0dB.

D. ANALYSIS BASED ON DIFFERENT OPTIMIZATION ALGORITHMS

The proposed mapping scheme based on GA is evaluated under the applications of PIP, MWD, 263enc mp3dec and mp3enc mp3dec, and the corresponding results are shown in Figure 19-a, -b, -c, and -d, respectively. The $OSNR_{WC}$ reaches the optimal values of 47.1dB, 44.6dB, 47.3dB, and 43.0dB, respectively. The results are the same with the ACO algorithm. It can be observed that either ACO-based or GA-based scheme is able to perform a reliable search and obtain an optimal result, even if multiple run times are required.

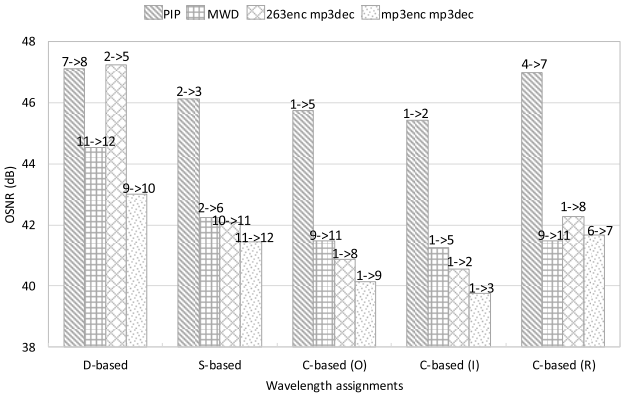

FIGURE 20. OSNR results with different wavelength assignments under different applications, i.e., PIP, MWD, 263enc mp3dec, and mp3enc mp3dec. "D-based" and "S-based" are short for destination-based wavelength assignment and source-based wavelength assignment. "C-based (O)", "C-based (I)", and "C-based (R)" are short for communication-based wavelength assignment with ordinal order, inverse order, and random order, separately.

To further ameliorate the proposed scheme, some improved versions of GA can also be adopted. For instance, the initial generation can be selected in combination with the ACO algorithm, which is not the focus of this work.

E. ANALYSIS OF WAVELENGTH ASSIGNMENT SCHEMES

Wavelength assignment also has a significant influence on communication reliability. All the above evaluation results are obtained with the destination-based wavelength assignment. In Figure 20, $OSNR_{WC}$ of the three wavelength assignment methods (i.e., destination-based wavelength assignment, source-based wavelength assignment, and communication-based wavelength assignment) are explored under different applications.

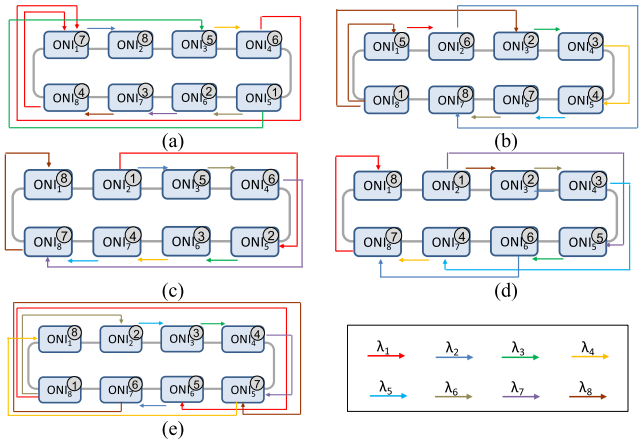

FIGURE 21. The mapping results under PIP application with different wavelength assignment schemes: a) destination-based; b) source-based; c) communication-based with ordinal order; d) communication-based with inverse order; e) communication-based with random order.

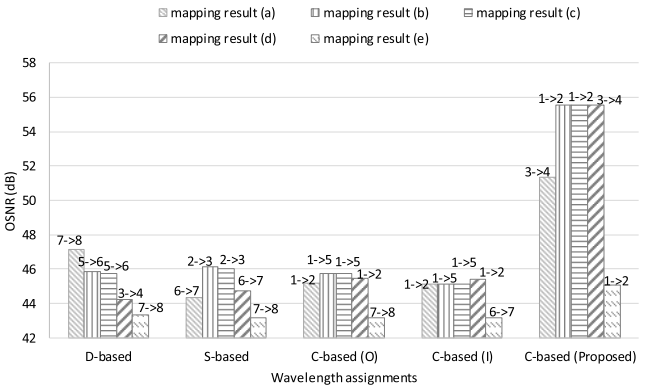

FIGURE 22. OSNR results with different wavelength assignment schemes, under the mapping results of PIP in Figure 21-a, -b, -c, -d, and e respectively. "D-based", "S-based", "C-based (O)", "C-based (I)", and " C-based (Proposed)" are short for the wavelength assignment schemes of destination-based, source-based, communication-based with ordinal order, communication-based with inverse order, and the proposed method using optimization algorithm, separately.

The evaluation results of destination-based wavelength assignment exhibit the biggest $OSNR_{WC}$, e.g., 47.1dB under PIP, while the communication-based wavelength assignment with inverse order gets the smallest $OSNR_{WC}$, e.g., 45.4dB under PIP. This is because some communications sharing the same destination cannot communication at the same time, resulting in less crosstalk. It is necessary to design a proper wavelength assignment scheme, to obtain a higher reliability and fulfill more communications at the same time. According to the results, the destination-based wavelength assignment always gets the highest $OSNR_{WC}$, and this is the reason why it is used in the previous analysis.

Meanwhile, different wavelength assignment schemes result in different mapping results, which may lead to different communication pairs corresponding to the $OSNR_{WC}$. As shown in Figure 20, "$i \rightarrow j$" represents the task cores corresponding to the $OSNR_{WC}$ of each case. For instance, "7→8" of "D-based" indicates that the communication from task core 7 to task core 8 obtains the optimal $OSNR_{WC}$ under PIP with the destination-based wavelength assignment. It also can be seen that under the same application, different wavelength assignment schemes correspond to different task cores with the $OSNR_{WC}$. That is because the optimal mapping results are different when the wavelength assignments are constrained. In addition, it illustrates that destination-based wavelength assignment contributes a better result of OSNR at this stage of application mapping under a same application. This is the reason why we utilize the destination-based wavelength assignment at Phase I of our proposed method.

The mapping results (in Figure 20) with different wavelength assignment schemes under PIP are given in Figure 21, together with the wavelength assignment results. For instance, the $OSNR_{WC}$ of "D-based" corresponds to the communication of task core 7→8, i.e., ONI 1→2 in the mapping result of Figure 21-a, with the assigned wavelength λ_1. The $OSNR_{WC}$ of "C-based (I)" corresponds to the communication of task core 1→2, i.e., ONI 2→3, with the assigned wavelength λ_8, as shown in Figure 21-d.

To further analyze the influence of wavelength assignment scheme, $OSNR_{WC}$ obtained by using the proposed mapping scheme is evaluated, along with other wavelength assignment schemes. The same application graph and same mapping result are considered, and the results of $OSNR_{WC}$ are shown in Figure 22. Under the same mapping result, the wavelength assignment by adopting the proposed method contributes the best $OSNR_{WC}$. For instance, "C-based (Proposed)" achieves an $OSNR_{WC}$ of 51.3dB, while "D-based" obtains 47.1dB under the same mapping result in Figure 21-a. Thus, the proposed wavelength assignment can achieve an improvement of 4.2dB at least, compared to the other wavelength assignment schemes.

It can be observed the different wavelength assignments not only perform differently on reliability results, but also lead to different corresponding communications. For instance, the $OSNR_{WC}$ of "C-based (Proposed)" corresponds to the communication of task core 3→4, while the $OSNR_{WC}$ of "D-based" corresponds to task core 7→8 under the same mapping result in Figure 21-a. It is assumed that only one wavelength is assigned to a communication, without the consideration of the communication weight. However, the communication with higher weight can be assigned with more than one wavelength, to increase the throughput and reduce the communication delay. This would be explored as a part of the future work, by considering a compromise between the reliability and the communication delay. Our method is designed to reach the result with higher reliability and less time. The reduced time is due to the reduction of the search space brought by both the optimization algorithm and the problem decomposition.

F. EXPLORATION ON THE WAVELENGTH CHANNELS

As shown in Figure 23, the communication reliability of the proposed method is further explored under different

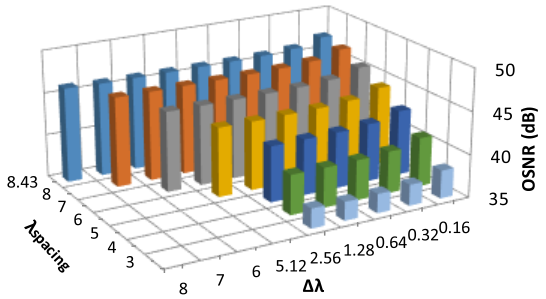

FIGURE 23. The communication reliability exploration with different wavelength spacings (i.e., $\lambda_{spacing}$) and wavelength drifts (i.e., $\Delta\lambda$) between ON and OFF state of MRs for the proposed scheme.

wavelength spacings (i.e., $\lambda_{spacing}$) between the adjacent wavelength channels, and under different wavelength drifts (i.e., $\Delta\lambda$) between the ON and OFF state of MR.

For the case of PIP mapped onto 8 ONIs, eight wavelengths are utilized for communication with the $\lambda_{spacing}$ of 8.43nm and $\Delta\lambda$ of 0.16nm [33]. The wavelength spacing will be smaller when more wavelength channels are used in the range of a given FSR, and the wavelength drifts will be different when the MRs are designed differently. The influence of these two factors on $OSNR_{WC}$ is investigated, ensuring the wavelength drift would not result in wavelength overlapping or disorder of wavelength channels. That is to say, the wavelength after drift from ON to OFF is still in the range of initial wavelength and the next wavelength channel. For instance, $\lambda_1+\Delta\lambda$ is smaller than λ_2, as shown in Figure 4. In the evaluation results, $OSNR_{WC}$ gets smaller as $\lambda_{spacing}$ decreases under the same $\Delta\lambda$. This is induced by the increasing crosstalk under a constant signal power. At the same time, OSNR gets smaller as $\Delta\lambda$ increases under the same $\lambda_{spacing}$. This is because the optical signal power keeps almost the same level while the crosstalk increases due to the smaller spacing between two adjacent wavelengths.

In addition, under a given FSR, the total number of available wavelengths is limited, since the spacing between two adjacent wavelengths would decrease as the number of wavelengths increases. Thus, more wavelengths correspond to increasing crosstalk and decreasing communication reliability. With the continuous increase of the number of communication pairs, it is not sufficient to support all the parallel communication pairs with just the strategy of reusing wavelengths. Other strategies are necessary to be considered for supporting the communication. For instance, spatial multiplexing by adding more waveguides in a given architecture can be used (for example in MRONoC [11]), so that the limited number of available wavelengths are reused in different waveguides to improve the communication performance.

Therefore, the number of wavelengths used for communication needs to be properly studied for the tradeoff of performance and reliability.

IX. CONCLUSION

In this paper, we propose a novel joint method to map the applications onto the network architecture, with the consideration of wavelength assignment to improve communication reliability. Two aspects, i.e., application mapping and wavelength assignment, are considered in this work. Different optimization algorithms, e.g., ACO and genetic algorithms, are applied and evaluated in the proposed method. This method is universal to employ different optimization algorithms. In the evaluation of accuracy and efficiency, different applications are considered in implementing the mapping with the proposed method. The influence of different wavelength assignment schemes is evaluated, and a reliability-aware wavelength assignment scheme is proposed to use to improve the reliability jointly. The evaluation results indicate that the mapping considering the wavelength assignment can lead to better reliability. The design space, e.g., the influence of the wavelength spacing between two adjacent wavelengths and the wavelength drift between ON and OFF state, is further studied. This work is mainly focused on the proposed reliability-aware joint design method. In the future, the work will be done in the aspects of the exploration of other efficient optimization algorithms, the design of run-time mapping scheme, and the application mapping considering the thermal effect.

REFERENCES

[1] A. Biberman and K. Bergman, "Optical interconnection networks for high-performance computing systems," *Rep. Prog. Phys.*, vol. 75, no. 4, Apr. 2012, Art. no. 046402.

[2] C. Sun *et al.*, "Single-chip microprocessor that communicates directly using light," *Nature*, vol. 528, no. 7583, pp. 534–538, Dec. 2015.

[3] A. H. Atabaki, S. Moazeni, F. Pavanello, H. Gevorgyan, J. Notaros, L. Alloatti, M. T. Wade, C. Sun, S. A. Kruger, H. Meng, K. Al Qubaisi, I. Wang, B. Zhang, A. Khilo, C. V. Baiocco, M. A. Popović, V. M. Stojanović, and R. J. Ram, "Integrating photonics with silicon nanoelectronics for the next generation of systems on a chip," *Nature*, vol. 556, no. 7701, pp. 349–354, Apr. 2018.

[4] S. Le Beux, H. Li, and G. Nicolescu, "Optical crossbars on chip, a comparative study based on worst-case losses," *Concurrency Comput., Pract. Exper.*, vol. 26, no. 15, pp. 2492–2503, 2014.

[5] F. Liu, H. Zhang, Y. Chen, Z. Huang, and H. Gu, "WRH-ONoC: A wavelength-reused hierarchical architecture for optical network on chips," in *Proc. IEEE Conf. Comput. Commun. (INFOCOM)*, Apr. 2015, pp. 1912–1920.

[6] H. Li, A. Fourmigue, S. Le Beux, I. O'Connor, and G. Nicolescu, "Towards maximum energy efficiency in nanophotonic interconnects with thermal-aware on-chip laser tuning," *IEEE Trans. Emerg. Topics Comput.*, vol. 6, no. 3, pp. 343–356, Jul. 2018.

[7] J. Luo, C. Killian, S. L. Beux, D. Chillet, O. Sentieys, and I. O'Connor, "Offline optimization of wavelength allocation and laser power in nanophotonic interconnects," *ACM J. Emerg. Technol. Comput. Syst.*, vol. 14, no. 2, pp. 1–19, Jul. 2018.

[8] E. Fusella and A. Cilardo, "Reducing power consumption of lasers in photonic NoCs through application-specific mapping," *ACM J. Emerg. Technol. Comput. Syst.*, vol. 14, no. 2, pp. 1–11, Jul. 2018.

[9] J. Luo, A. Elantably, V. D. Pham, C. Killian, D. Chillet, S. Le Beux, O. Sentieys, and I. O'Connor, "Performance and energy aware wavelength allocation on ring-based WDM 3D optical NoC," in *Proc. Design, Autom. Test Eur. Conf. Exhib. (DATE)*, Mar. 2017, pp. 1372–1377.

[10] M. Bahadori, S. Rumley, H. Jayatilleka, K. Murray, N. A. F. Jaeger, L. Chrostowski, S. Shekhar, and K. Bergman, "Crosstalk penalty in microring-based silicon photonic interconnect systems," *J. Lightw. Technol.*, vol. 34, no. 17, pp. 4043–4052, Sep. 1, 2016.

[11] H. Gu, K. Chen, Y. Yang, Z. Chen, and B. Zhang, "MRONoC: A low latency and energy efficient on chip optical interconnect architecture," *IEEE Photon. J.*, vol. 9, no. 1, pp. 1–12, Feb. 2017, doi: 10.1109/JPHOT.2017.2651586.

[12] L. H. K. Duong, M. Nikdast, S. Le Beux, J. Xu, X. Wu, Z. Wang, and P. Yang, "A case study of Signal-to-Noise ratio in ring-based optical networks-on-chip," *IEEE Des. Test. Comput.*, vol. 31, no. 5, pp. 55–65, Oct. 2014.

[13] M. Nikdast, J. Xu, L. H. K. Duong, X. Wu, X. Wang, Z. Wang, Z. Wang, P. Yang, Y. Ye, and Q. Hao, "Crosstalk noise in WDM-based optical networks-on-chip: A formal study and comparison," *IEEE Trans. Very Large Scale Integr. (VLSI) Syst.*, vol. 23, no. 11, pp. 2552–2565, Nov. 2015.

[14] Y. Xie, M. Nikdast, J. Xu, X. Wu, W. Zhang, Y. Ye, X. Wang, Z. Wang, and W. Liu, "Formal worst-case analysis of crosstalk noise in mesh-based optical networks-on-chip," *IEEE Trans. Very Large Scale Integr. (VLSI) Syst.*, vol. 21, no. 10, pp. 1823–1836, Oct. 2013.

[15] M. Nikdast, J. Xu, and X. Wu, "Systematic analysis of crosstalk noise in folded-torus-based optical networks-on-chip," *IEEE Trans. Comput.-Aided Design Integr. Circuits Syst.*, vol. 33, no. 3, pp. 437–450, Feb. 2014.

[16] M. Nikdast, J. Xu, L. H. K. Duong, X. Wu, Z. Wang, X. Wang, and Z. Wang, "Fat-tree-based optical interconnection networks under crosstalk noise constraint," *IEEE Trans. Very Large Scale Integr. (VLSI) Syst.*, vol. 23, no. 1, pp. 156–169, Jan. 2015.

[17] Y. Xie, M. Nikdast, J. Xu, W. Zhang, Q. Li, X. Wu, Y. Ye, X. Wang, and W. Liu, "Crosstalk noise and bit error rate analysis for optical network-on-chip," in *Proc. 47th Design Autom. Conf. (DAC)*, 2010, pp. 657–660.

[18] J. H. Lee and T. H. Han, "Wavelength-based crosstalk-aware design for hybrid optical network-on-chip," *Opt. Eng.*, vol. 56, no. 1, Jan. 2017, Art. no. 016111.

[19] Z. Li, M. Mohamed, X. Chen, E. Dudley, K. Meng, L. Shang, A. R. Mickelson, R. Joseph, M. Vachharajani, B. Schwartz, and Y. Sun, "Reliability modeling and management of nanophotonic on-chip networks," *IEEE Trans. Very Large Scale Integr. (VLSI) Syst.*, vol. 20, no. 1, pp. 98–111, Jan. 2012.

[20] E. Fusella and A. Cilardo, "Crosstalk-aware mapping for tile-based optical network-on-chip," in *Proc. IEEE 17th Int. Conf. High Perform. Comput. Commun., 7th Int. Symp. Cyberspace Saf. Secur., IEEE 12th Int. Conf. Embedded Softw. Syst.*, Aug. 2015, pp. 1139–1142.

[21] E. Fusella and A. Cilardo, "Crosstalk-aware automated mapping for optical networks-on-chip," *ACM Trans. Embedded Comput. Syst.*, vol. 16, no. 1, pp. 1–26, Nov. 2016.

[22] L. H. K. Duong, P. Yang, Z. Wang, Y.-S. Chang, J. Xu, Z. Wang, and X. Chen, "Crosstalk noise reduction through adaptive power control in inter/intra-chip optical networks," *IEEE Trans. Comput.-Aided Design Integr. Circuits Syst.*, vol. 38, no. 1, pp. 43–56, Jan. 2019.

[23] S. V. R. Chittamuru, I. G. Thakkar, and S. Pasricha, "HYDRA: Heterodyne crosstalk mitigation with double microring resonators and data encoding for photonic NoCs," *IEEE Trans. Very Large Scale Integr. (VLSI) Syst.*, vol. 26, no. 1, pp. 168–181, Jan. 2018.

[24] I. G. Thakkar, S. V. R. Chittamuru, and S. Pasricha, "Improving the reliability and energy-efficiency of high-bandwidth photonic NoC architectures with multilevel signaling," in *Proc. 11th IEEE/ACM Int. Symp. Netw. Chip*, Oct. 2017, pp. 1–8.

[25] S. V. R. Chittamuru and S. Pasricha, "Improving crosstalk resilience with wavelength spacing in photonic crossbar-based network-on-chip architectures," in *Proc. IEEE 58th Int. Midwest Symp. Circuits Syst. (MWSCAS)*, Fort Collins, CO, USA, Aug. 2015, pp. 1–4.

[26] P. Bogdan, T. Dumitraş, and R. Marculescu, "Stochastic communication: A new paradigm for fault-tolerant networks-on-chip," *VLSI Design special issue Networks-on-Chip*, vol. 2007, Apr. 2007, Art. no. 95348.

[27] Y. Xue and P. Bogdan, "User cooperation network coding approach for NoC performance improvement," in *Proc. 9th Int. Symp. Netw. Chip (NOCS)*, 2015, pp. 1–8.

[28] Y. Xue and P. Bogdan, "Improving NoC performance under spatio-temporal variability by runtime reconfiguration: A general mathematical framework," in *Proc. 10th IEEE/ACM Int. Symp. Networks-on-Chip (NOCS)*, Sep. 2016, pp. 1–8.

[29] X. Wang, H. Gu, Y. Yang, K. Wang, and Q. Hao, "RPNoC: A ring-based packet-switched optical Network-on-Chip," *IEEE Photon. Technol. Lett.*, vol. 27, no. 4, pp. 423–426, Feb. 2015, doi: 10.1109/LPT.2014.2376972.

[30] S. L. Beux, H. Li, I. O'Connor, K. Cheshmi, X. Liu, J. Trajkovic, and G. Nicolescu, "Chameleon: Channel efficient optical network-on-chip," in *Proc. Design, Autom. Test Eur. Conf. Exhib. (DATE)*, 2014, pp. 1–6.

[31] L. Ramini, P. Grani, S. Bartolini, and D. Bertozzi, "Contrasting wavelength-routed optical NoC topologies for power-efficient 3D-stacked multicore processors using physical-layer analysis," in *Proc. Design, Autom. Test Eur. Conf. Exhib. (DATE)*, 2013, pp. 1589–1594.

[32] J. Psota, J. Miller, G. Kurian, H. Hoffman, N. Beckmann, J. Eastep, and A. Agarwal, "ATAC: Improving performance and programmability with on-chip optical networks," in *Proc. IEEE Int. Symp. Circuits Syst.*, May 2010, pp. 3325–3328.

[33] H. Li, S. Le Beux, Y. Thonnart, and I. O'Connor, "Complementary communication path for energy efficient on-chip optical interconnects," in *Proc. 52nd Annu. Design Autom. Conf. (DAC)*, San Francisco, CA, USA, Jun. 2015, pp. 1–6.

[34] T. Stützle and H. H. Hoos, "MAX-MIN ant system," *Future Generat. Comput. Syst.*, vol. 16, no. 8, pp. 889–914, Jun. 2000.

[35] G. N. Varela and M. C. Sinclair, "Ant colony optimisation for virtual-wavelength-path routing and wavelength allocation," in *Proc. Congr. Evol. Comput. (CEC)*, 1999, pp. 1809–1816.

[36] S. Khan, S. Anjum, U. A. Gulzari, F. Ishmanov, M. Palesi, and M. K. Afzal, "An optimized hybrid algorithm in term of energy and performance for mapping real time workloads on 2D based on-chip networks," *Int. J. Speech Technol.*, vol. 48, no. 12, pp. 4792–4804, Dec. 2018.

[37] Z. Chu, H. Li, H. Gu, and X. Ye, "Wavelength assignment method based on ACO to reduce crosstalk for ring-based optical network-on-chip," *Microprocessors Microsyst.*, vol. 71, Nov. 2019, Art. no. 102849.

[38] R. A. Barry and P. A. Humblet, "Latin routers, design and implementation," *J. Lightw. Technol.*, vol. 11, nos. 5–6, pp. 891–899, May 1993.

[39] P. K. Sahu and S. Chattopadhyay, "A survey on application mapping strategies for network-on-chip design," *J. Syst. Archit.*, vol. 59, no. 1, pp. 60–76, Jan. 2013.

[40] E. Fusella and A. Cilardo, "PhoNoCMap: An application mapping tool for photonic Networks-on-Chip," in *Proc. Design, Autom. Test Eur. Conf. Exhib. (DATE)*, 2016, pp. 289–292.

[41] S. Murali and G. De Micheli, "Bandwidth-constrained mapping of cores onto NoC architectures," in *Proc. Design, Autom. Test Eur. Conf. Exhib.*, 2004, pp. 896–901.

[42] J. Hu and R. Marculescu, "Energy-aware mapping for tile-based NoC architectures under performance constraints," in *Proc. Conf. Asia South Pacific design Autom. (ASPDAC)*, 2003, pp. 233–239.

[43] Y. Xue and P. Bogdan, "Scalable and realistic benchmark synthesis for efficient NoC performance evaluation: A complex network analysis approach," in *Proc. 11th IEEE/ACM/IFIP Int. Conf. Hardw./Softw. Codesign Syst. Synth. (CODES)*, Oct. 2016, pp. 1–10.

[44] Y. Xiao, Y. Xue, S. Nazarian, and P. Bogdan, "A load balancing inspired optimization framework for exascale multicore systems: A complex networks approach," in *Proc. IEEE/ACM Int. Conf. Comput.-Aided Design (ICCAD)*, Nov. 2017, pp. 217–224.

[45] Y. Xiao, S. Nazarian, and P. Bogdan, "Self-optimizing and self-programming computing systems: A combined compiler, complex networks, and machine learning approach," *IEEE Trans. Very Large Scale Integr. (VLSI) Syst.*, vol. 27, no. 6, pp. 1416–1427, Jun. 2019.

[46] M. H. Mottaghi and H. R. Zarandi, "DFTS: A dynamic fault-tolerant scheduling for real-time tasks in multicore processors," *Microprocessors Microsyst.*, vol. 38, no. 1, pp. 88–97, Feb. 2014.

[47] F. Ferrandi, P. L. Lanzi, C. Pilato, D. Sciuto, and A. Tumeo, "Ant colony heuristic for mapping and scheduling tasks and communications on heterogeneous embedded systems," *IEEE Trans. Comput.-Aided Design Integr. Circuits Syst.*, vol. 29, no. 6, pp. 911–924, Jun. 2010.

[48] E. Fusella and A. Cilardo, "Minimizing power loss in optical networks-on-chip through application-specific mapping," *Microprocessors Microsyst.*, vol. 43, pp. 4–13, Jun. 2016.

HUI LI (Member, IEEE) received the Ph.D. degree in electronics, micro- and nano-electronics, optics and laser from Ecole Centrale de Lyon, France, in 2017. She is currently a Lecturer with the State Key Laboratory of Integrated Services Networks, School of Telecommunications Engineering, Xidian University, China. Her research interests include emerging interconnects for different applications, such as on-chip, data center, and supercomputing.

FEIYANG LIU received the Ph.D. degree from the University of Otago, New Zealand, in December 2017. He is currently a Research Engineer from the Xi'an Aeronautics Computing Technique Research Institute, AVIC, China. His research interests include network on chip (NoC), optical network on chip (ONoC), avionics, and deep neural network accelerators.

HUAXI GU is currently a Full Professor with the State Key Lab, ISN, Xidian University. He is also the Principal Investigator of one key, two general, and one youth project from National Natural Science Foundation of China. He is also PI of the joint projects with Intel Labs China, Shannon Lab (HUAWEI), Communication Technology Lab (Huawei), ZTE, and CETC. He has published more than 160 journal and conference papers. He has applied for more than 40 Chinese patents, with 20 patents granted. His research interests include networking technologies, network on chip, and optical interconnect. He has served as a TPC Member of GLOBECOM2017and PDCAT2016 and the Technical Reviewer for multiple journals, including the IEEE TRANSACTIONS ON COMPUTER, the IEEE TRANSACTIONS ON VLSI, the IEEE TRANSACTIONS ON CLOUD COMPUTING, the IEEE/OSA JOURNAL OF LIGHTWAVE TECHNOLOGY, and INFOCOM2016. He received the Second Prize of the National Science and Technology Progress Award, in 2016, and the First Prize of Science and Technology Award of Shaanxi Province, in 2015. He received the Best Paper Honorable Mention Award from the IEEE ISVLSI2009 and the Best Paper Award from ACM TURC 2017(SIGCOMM China).

ZHUQIN CHU received the B.E. degree in applied mathematics from Xidian University, in 2017, where she is currently pursuing the M.E. degree in telecommunication and information systems with the State key Lab of ISN. Her main research interests include network-on-chip and optical interconnected networks.

XIAOCHUN YE is currently an Associate Researcher with the High-throughput Computer Research Center, Institute of Computing Technology, Chinese Academy of Sciences, China. He is mainly involved in the research of many nuclear processor structures. As a core backbone, he has participated in the development of Godson-T high-performance many-core processor and DPU high-throughput many-core processor. In recent years, he has published more than 60 articles in the field of computer architecture, more than 20 authorized/received domestic/international invention patents. As the person in charge or the backbone, he participated in more than ten projects, such as 973, 863, National Key Research and Development Program, Fund Key/Face, Nuclear High Base, and Chinese Academy of Sciences Pilot A. He won the Second Prize of the Beijing Science and Technology Award, the Science and Technology Achievement Transformation Award of the Chinese Academy of Sciences, and the Wu Wenjun Artificial Intelligence Technology Invention Award.